

# Reviews

## Conducting Polymer Nanocomposites: A Brief Overview

Rupali Gangopadhyay and Amitabha De\*

*Chemical Sciences Division, Saha Institute of Nuclear Physics, 1/AF, Bidhannagar, Calcutta 700 064, India*

*Received August 18, 1999*

Inorganic nanoparticles of different nature and size can be combined with the conducting polymers, giving rise to a host of nanocomposites with interesting physical properties and important application potential. Such nanocomposites have been discussed in this review, throwing light on their synthesis techniques, properties, and applications. A large variety of nanoparticles have been chosen in this respect with inclusion techniques utilizing both chemical and electrochemical routes. The nature of the association between the components can be studied from TEM pictures. Depending upon the synthesis techniques and the characteristics of the inorganic materials, ultimate properties of the resulting composite are controlled. In this way, the exceptional colloidal stability of different silica sols have been utilized to form stable PPy-silica and PAN-silica nanocomposite colloids. Similarly the magnetic susceptibility of  $\gamma$ -Fe<sub>2</sub>O<sub>3</sub>, the electrochromic property of WO<sub>3</sub>, and the catalytic activity of Pd, Pt, etc. metals have been successfully combined with existing electrical conductivity of conducting polymers in the hybrid nanocomposite materials. Functional groups viz. -NH<sub>2</sub> and -COOH have also been added to the composite particles and all these combinations and modifications have improved the applicability of conducting polymers in different fields, e.g., electrodes of batteries, display devices, immunodiagnostic assay, etc.

### Contents

I. Introduction	608
II. Chemical Preparations	610
1. Nanocomposites in Stable Colloidal Form	610
2. Nanocomposites with Improved Physical, Mechanical, and Electrical Properties	612
3. Nanocomposites with Magnetic Susceptibility	614
4. Nanocomposites with Dielectric Property, Energy Storage, and Catalytic Activity	616
5. Nanocomposites with Surface Functionalized Core and/or Shell	617
III. Electrochemical Preparations	619
1. Nanocomposites with Charge Storage and Electrochromic Activities	619
2. Nanocomposites with Catalytic Properties	620
3. Nanocomposites with Magnetic Susceptibility	621
IV. Conclusion	621

### I. Introduction

Progress in the field of materials science has taken a new lead since the advent of the nanocluster-based

materials or nanocomposites. Nanoclusters are ultrafine particles of nanometer dimensions and whose characteristics are size dependent and are different from those of the atomic and bulk counterparts. Nanocomposites are a special class of materials originating from suitable combinations of two or more such nanoparticles or nanosized objects in some suitable technique, resulting in materials having unique physical properties and wide application potential in diverse areas. Novel properties of nanocomposites can be derived from the successful combination of the characteristics of parent constituents into a single material. Materials scientists very often handle such nanocomposites, which are an effective combination of two or more inorganic nanoparticles. To exploit the full potential of the technological applications of the nanomaterials, it is very important to endow them with good processability which has ultimately guided scientists toward using conventional polymers as one component of the nanocomposites, resulting in a special class of hybrid materials termed "polymeric nanocomposites". These materials are also intimate combinations (up to almost molecular level) of one or more inorganic nanoparticles with a polymer so that unique properties of the former can be taken together with the existing qualities of the latter. Many investigations<sup>1</sup> regarding the development of the incorporation techniques of the nanoparticles into the polymeric matrices have been published. In most of the cases<sup>2</sup> such combinations require blending or mixing of the components, taking the polymer in solution or in melt form. Resulting

**Table 1. Conducting Polymer Nanocomposites at a Glance<sup>a</sup>**

nanocomposite of interest		significant characterization/applications	ref(s)
polymer (shell)	inorganic particle (core)		
PPy and PAN	SiO <sub>2</sub> (1 μm, ~35 nm, 20 nm), SnO <sub>2</sub> -Sb (10 nm), stringy SiO <sub>2</sub> (40–300 nm long)	nanocomposites in stable colloidal form, showing “raspberry” morphology and inorganic particle rich surface	9–22
PPy and PAN	CeO <sub>2</sub> (0.52 μm), CuO (1.6 μm), α-Fe <sub>2</sub> O <sub>3</sub> (spherical, polyhedral and spindle shaped), NiO (3.8 μm), SiO <sub>2</sub> (0.46 μm)	colloidally stable nanocomposite having extremely low dc conductivity was formed without using any polymerization initiator	23–26
PPy and PAN	BaSO <sub>4</sub> (20 nm), colloidal gold with particles 7–9 nm and Al <sub>2</sub> O <sub>3</sub> membrane	in situ formation of colloidal nanocomposite within the microemulsion or inside the Al <sub>2</sub> O <sub>3</sub> membrane	27–30
PPy, PAN, NVC, and PPV	ZrO <sub>2</sub> (20–30 nm), Fe <sub>2</sub> O <sub>3</sub> (25–50 nm), SiO <sub>2</sub> , n-TiO <sub>2</sub> (~10 nm), Al <sub>2</sub> O <sub>3</sub> (35–50 nm), MgO (2–4 μm), CB	nanocomposites in macroscopic precipitate form or with limited colloidal stability but improved thermal and electrical properties and novel transport properties	31–37
PPy and PAOABSA	MS (5–30 nm), Fe <sub>3</sub> O <sub>4</sub> (14 nm), Fe <sub>2</sub> O <sub>3</sub> (15–50 nm), γ-Fe <sub>2</sub> O <sub>3</sub> (~85 nm)	nanocomposites with significant magnetic susceptibility	38–47, 93–95
PPy and PAN	BT (~1 μm), LiMnO <sub>2</sub> , LiMn <sub>2</sub> O <sub>4</sub> , V <sub>2</sub> O <sub>5</sub> , β-MnO <sub>2</sub> , PMO <sub>12</sub> , H <sub>3</sub> PMo <sub>12</sub> O <sub>40</sub> , CB, Fe <sub>2</sub> O <sub>3</sub> (4 nm, 40 nm)	nanocomposites with important charge storage and dielectric properties; materials suitable for cathode applications	48–52, 79–84
PPy, PAN, PTh, and PEDOT	Pt (~4 nm), PtO <sub>2</sub> , Pt, Cu, Pd, SiO <sub>2</sub> (20 nm) and bimetallic couples	nanocomposites containing catalytically important metals; important for catalytic applications	53–58, 88–92
PPy and PAN	SiO <sub>2</sub> (20 nm)	surface functionalized nanocomposites; important for immunodiagnostic assays	59–72
PPy	SiO <sub>2</sub> , PB, MnO <sub>2</sub> , Ta <sub>2</sub> O <sub>5</sub> , TiO <sub>2</sub>	electrochemically synthesized composite films having improved charge storage properties	73–78
PPy and PAN	WO <sub>3</sub>	nanocomposite films with important ECD application and optical activity	85–87

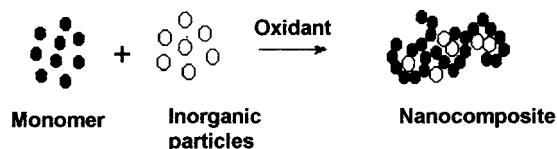
<sup>a</sup> Nonconducting and template-guided nanocomposites (refs 1–8) are not included.

nanocomposites have found successful applications in versatile fields viz. battery cathodes,<sup>3</sup> microelectronics,<sup>4</sup> nonlinear optics,<sup>5</sup> sensors,<sup>6</sup> etc.

The perspective is somewhat different with the inherently conducting polymers (ICP). These conjugated conducting polymers are infusible in nature and are generally insoluble in common solvents. Such inherent intractability has prevented the ICPs from combining with the foreign materials in conventional blending techniques to form nanocomposite. Therefore, synthesis techniques had to be found and optimized to incorporate the inorganic component into the conducting polymer; this added a separate dimension to the nanocomposite research. In the conventional nanocomposites, the polymer adds flexibility to the system and improves processability to a large extent. In conducting polymer nanocomposites, on the other hand, the nanoparticles generally provide the system with some kind of processability (colloidal stability or mechanical strength), although the specific properties of the latter are also utilized in some respects.

Inorganic materials used for this purpose are generally of two types: nanoparticles and some nanostructured materials or templates. Depending upon the nature of association between the inorganic and organic components, nanocomposites are also classified into two categories: one in which the inorganic particle is embedded in organic matrix and the other where organic polymer is confined into inorganic template. However, in each case the composite formation demands some entrapment or encapsulation (Scheme 1) rather than simple blending or mixing. This review focuses on the former class of composite, introduced here as the “inorganic-in-organic” system. Such nanocomposites not only bridge the world of microparticles with that of the macromolecules, but often makes successful strides toward overcoming the processing problems of ICPs

### Scheme 1. Formation of Nanocomposite from the Constituents



which have enhanced their importance to a large extent. Template-guided composites have also occupied a very large area in the world of nanocomposites. In fact investigations regarding the ICP nanocomposites started with the template-guided systems and later they have come out as advanced materials with good processability and widespread application potential. These materials have previously been peer reviewed<sup>7,8a,b</sup> several times and are therefore kept outside the scope of the present discussion.

Inorganic nanoparticles can be introduced into the matrix of a host-conducting polymer either by some suitable chemical route or by an electrochemical incorporation technique. These two synthesis techniques have given birth to materials that are widely different from one another in common physical properties and should therefore be discussed separately. However, each synthesis route opens a way to a group of materials with complementary behavior between two components. Chemical origins as well as the special properties of the incorporated materials viz. its catalytic property, magnetic susceptibility, colloidal stability, etc. always add new dimensions to the characteristics of the resulting composites and have accordingly divided them into different subgroups. For each particular system progress has been chronologically discussed since the pioneering works. Ongoing developments and promises are also discussed and suitable applications are mentioned. Table 1 summarizes the different ways of synthesizing

**Table 2. Categorizations of Conducting Polymer Nanocomposites**

Conducting Polymer Nanocomposites	
Inorganic-in-organic	Organic-in-inorganic
Chemical preparation	Electrochemical preparation
<ol style="list-style-type: none"> <li>1. Nanocomposites with colloidal stability (SiO<sub>2</sub>, SnO<sub>2</sub>, BaSO<sub>4</sub> etc. as core materials).</li> <li>2. Nanocomposites with improved physical and mechanical properties (Fe<sub>2</sub>O<sub>3</sub>, ZrO<sub>2</sub>, TiO<sub>2</sub> etc. as incorporated materials).</li> <li>3. Nanocomposites with magnetic susceptibility (using Fe<sub>3</sub>O<sub>4</sub>, γ-Fe<sub>2</sub>O<sub>3</sub> etc. magnetic particles).</li> <li>4. Nanocomposites with dielectric, energy storage, piezoresistive and catalytic activities (with BT, POM, PtO<sub>2</sub>, TiO<sub>2</sub>, Pd, Pt etc. incorporation).</li> <li>5. Nanocomposites with surface functionalization (-NH<sub>2</sub>/-COOH functional groups on surface and colloidal silica as core).</li> </ol>	<ol style="list-style-type: none"> <li>1. Nanocomposites with charge storage, optical and electrochromic activities (incorporation of MnO<sub>2</sub>, SnO<sub>2</sub>, CB, PB, WO<sub>3</sub>, SiO<sub>2</sub> etc.)</li> <li>2. Nanocomposites with catalytic activities (incorporation of catalytically active Pt, Pd, Cu etc. microparticles and some bimetallic couples like Pd/Cu etc.)</li> <li>3. Nanocomposites with magnetic susceptibility (γ-Fe<sub>2</sub>O<sub>3</sub>, magnetic macroanion).</li> </ol>

nanocomposites using different inorganic materials and conducting polymers with their respective properties, and applications with corresponding references, and Table 2 shows relevant categorization of the nanocomposites as followed here.

## II. Chemical Preparations

### 1. Nanocomposites in Stable Colloidal Form.

Encapsulation of inorganic particles inside the core of conducting polymers has become the most popular and interesting aspect of nanocomposite synthesis. A number of different metal and metal oxide particles have so far been encapsulated into the core of conducting polymers giving rise to a host of nanocomposites. These materials differ from the pure polymers in some of the physical and chemical properties and at the same time differ from each other also. Primarily, the objective of the work was to keep the polymer in a stable colloidal form and the stream of investigation was pioneered by Armes et al.<sup>9</sup> when they succeeded in incorporating large silica particles (diameter ~1 μm) into the core of polyaniline (PAn) and polypyrrole (PPy). Aniline was polymerized by (NH<sub>4</sub>)<sub>2</sub> S<sub>2</sub>O<sub>8</sub> (APS) in HCl while FeCl<sub>3</sub>·6H<sub>2</sub>O and salicylic acid were used for pyrrole. Polymerization of the respective monomers in the presence of the preformed colloids at low concentrations of monomer and oxidant was the key to synthesizing two stable colloids. This technique aims at slowing down the rate as well as the degree of polymerization and promotes the polymerization on the surface rather than in bulk. In effect, conducting polymer-SiO<sub>2</sub> colloids having PPy and PAn fraction of 5.73% and 3.73%, respectively, were obtained with electrical conductivity values  $2 \times 10^{-5}$  and  $4 \times 10^{-3}$  S/cm, respectively. Interestingly, the composites could be redispersed in solvents in which the outer PAn layer is soluble to some extent. Therefore, unlike the PPy-silica system, the polyaniline composite, in its doped form, could be

redispersed in concentrated H<sub>2</sub> SO<sub>4</sub> while in dedoped form it was dispersible in DMF. Repeating the experiment with PAn and smaller SiO<sub>2</sub> particles ( $38 \pm 7$  nm) stable colloid<sup>10,11a,b</sup> was formed where an optimum concentration of SiO<sub>2</sub> (2.0–2.3% w/v) colloid was required. The weight fraction of the polymer in the composites remained effectively constant (~21%). High mass loading of SiO<sub>2</sub> in these composites was best explained by assuming that the composite particles act as separate clusters of SiO<sub>2</sub> particles held together by the polymer component acting here as a bridging flocculant or binder. A high-resolution TEM picture obtained by Gill et al. was the first report to reveal an unusual “raspberry” morphology where the inorganic particles were “glued” with the chains of PAn. Composite particles were polydisperse in nature with an average particle diameter of 1.5–3.0 μm. Small-angle X-ray Scattering (SAXS) studies have revealed<sup>12</sup> that silica particles are 0.4 μm apart from one another which suggests polyaniline to be adsorbed onto the surface of silica particles as a thin layer of individual polymer chains. The same technique was repeated by Maeda et al.<sup>13,14</sup> for synthesizing stable PPy-SiO<sub>2</sub> colloid using 20 nm SiO<sub>2</sub> particles as dispersant. The critical SiO<sub>2</sub> concentration was kept at ~1.0% and fraction of PPy (%) in the composites varied from ~37% to ~70% depending upon the reaction parameters. A good solid-state conductivity (4 S/cm) was obtained and characteristic “raspberry” morphology was observed from TEM. A separation of 5–10 nm between SiO<sub>2</sub> particles, indicating the presence of a thinner layer, possibly a monolayer of PPy on SiO<sub>2</sub> particles was observed here, which indicates an almost molecular level dispersion of the components.

Whether such unique dispersing ability of the SiO<sub>2</sub> sol is due to any unique surface feature of SiO<sub>2</sub> or can be accounted only for large surface area of the sol has been investigated by Maeda and Armes. In their later publications,<sup>15,16</sup> they tried a broad spectrum of metal oxide colloids viz. SiO<sub>2</sub>, SnO<sub>2</sub> (pristine and antimony doped), TiO<sub>2</sub>, Sb<sub>2</sub>O<sub>3</sub>, ZrO<sub>2</sub>, and Y<sub>2</sub>O<sub>3</sub> for synthesizing PPy-based colloidal nanocomposites. But except for the SiO<sub>2</sub> and SnO<sub>2</sub> (both forms), the other four colloids failed to prevent macroscopic precipitation of the resulting nanocomposites. BET specific surface areas for the SiO<sub>2</sub>, SnO<sub>2</sub>, and SnO<sub>2</sub> (Sb) colloids were measured to be 129, 112, and 165 m<sup>2</sup>/g with an average particle size of 20, 8, and 10 nm, respectively. Relatively lower amounts (1.0–3.4 g) of these colloids were required for successful stabilization of PPy. On the other hand, other four oxides, despite having a larger particle size (up to 50 nm) and surface area (200 m<sup>2</sup> in total), failed to form colloid. This observation stresses the idea that a colloid with larger surface area is a necessary, but not sufficient, condition for formation of colloidal nanocomposite. PPy content in both types of SnO<sub>2</sub> (pristine and Sb doped) supported colloids were nearly equal but the electrical conductivity value in the latter sample was much higher (4–7 S/cm) as compared to the former (0.9 S/cm). The characteristic “raspberry” morphology (Figure 1) was found to be present in the TEM images of these systems also. Changing the structure of SiO<sub>2</sub> from spherical to elongated<sup>17</sup> (40–300 nm long and 5–20 nm in diameter) did not hamper the colloid formation. The

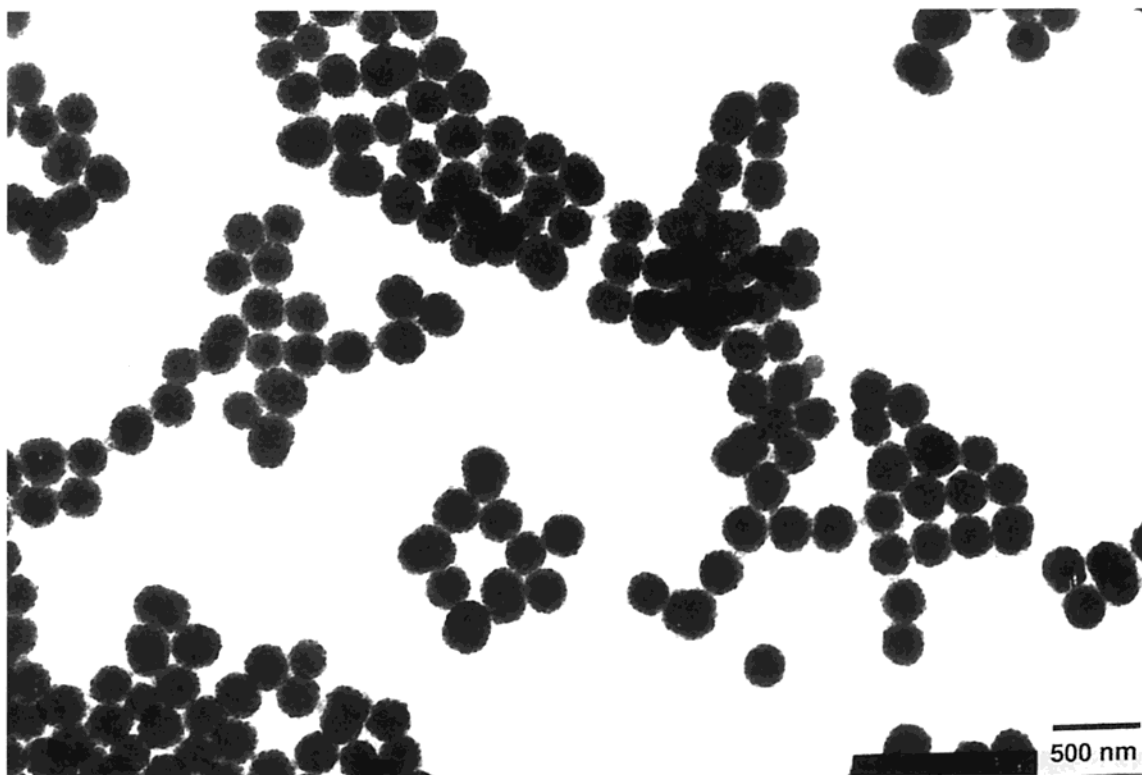


**Figure 1.** Transmission electron micrograph of a dilute dispersion of a PPy-silica colloidal nanocomposite. (Reproduced with permission from ref 21a. Copyright 1995 Academic Press.)

stringy silica colloid belongs to a larger specific surface area of  $200 \text{ m}^2/\text{g}$  but the minimum concentration required for colloid synthesis was only 0.8–0.9 w/v % which provides a total surface area of 160–180  $\text{m}^2$  in fair agreement with that obtained with spherical  $\text{SiO}_2$  ( $172 \text{ m}^2$ ). An optimum 0.9 w/v %  $\text{SiO}_2$  loading resulted in a PPy fraction of 55% and an electrical conductivity value of 3 S/cm. However, resistance of these  $\text{SiO}_2$  sols toward electrolyte-induced flocculation can account for their the unique efficiency in this respect; the other oxide sols lack such ability. BET surface area measurements on a group of 12 nanocomposites with the raspberry morphology including six PPy- $\text{SiO}_2$  composites, four PPy- $\text{SnO}_2$ , and two PAn- $\text{SiO}_2$ <sup>18</sup> have revealed that most of them possess significant porosity. Therefore, their specific surface area is always significantly larger than expected. Surface energy values calculated over a series of three composites i.e., PPy(Cl)- $\text{SiO}_2$ , PPy(Ts)- $\text{SiO}_2$ , and PPy( $\text{SO}_4$ )- $\text{SiO}_2$  obtained from Inverse gas chromatograph<sup>19</sup> data also imply microporosity in such materials, with high surface energy and heat of absorption. These composites were further characterized with XPS and  $\zeta$  potential measurements. The former<sup>20</sup> revealed that for the nanocomposites with higher colloidal stability, Si/N ratio at the surface was significantly higher than in the bulk, which indicates that the surface was silica rich rather than polymer rich. These very special surface characteristics provided them with prolonged colloidal stability comparable to the pure silica sol. This result was further supported by electrophoretic<sup>21a</sup> studies which revealed that electrokinetic behavior of the nanocomposite particles was mainly governed by the inorganic oxide component. Isoelectric point (IEP) of these composite particles was found to be almost equal to those of the bare particles. Therefore,

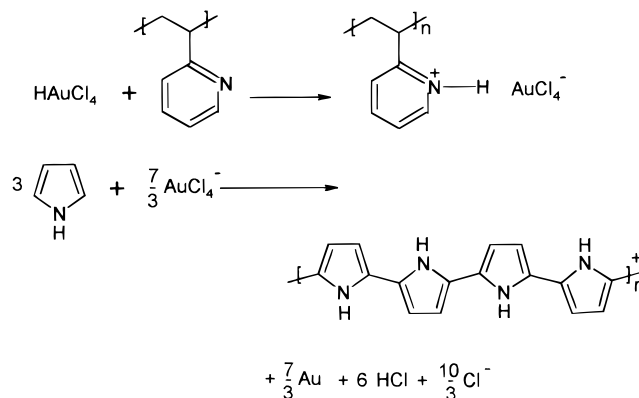
all these composites, to a first approximation, can be considered to be charge-stabilized large particles of the respective inorganic materials ( $\text{SiO}_2$  and  $\text{SnO}_2$ ) held by the polymer chains. In a recent publication Lascelles et al.<sup>21b</sup> have investigated the effect of several synthesis parameters viz. reaction temperature, reagent concentration, diameter and concentration of silica, nature of oxidant and stirring rate on the particle size, polymer content, and conductivity of PPy- $\text{SiO}_2$  nanocomposites. In contrast to their previous publication, here the nature of oxidant, concentration and diameter of silica, and polymerization temperature was found to have no effect on particle size and chemical composition of the nanocomposites while the rate of stirring was of some importance. Colloidal stability, however, was dependent on silica concentration and nature of oxidant to some extent. The larger surface area of the nanocomposites have offered them better performance as a bioadsorbent as compared to the pure polymer (PPy). In a very recent report,<sup>22</sup> both the PPy( $\text{SO}_4$ )- $\text{SiO}_2$  nanocomposite and the pure PPy( $\text{SO}_4$ ) were allowed to adsorb a model protein, human serum albumin (HSA), and spectrophotometric methods have revealed that colloidal nanocomposites are much more adsorptive toward HSA, especially where a higher HSA concentration is maintained.

The general synthesis route for such hybrid nanocomposite materials is to polymerize aniline or pyrrole in the presence of some preformed inorganic particles, using an appropriate soluble oxidant. This technique was slightly modified by Matijevec et al. who have dropped the last item in their work. In a series of their publications the synthesis and characterization of a good number of colloidal nanocomposites have been reported applying a host of inorganic oxides as core materials. But instead of using an oxidizing agent, they have

rather utilized the catalytic activity of the core surfaces, often after some modification or activation, for polymerization of the respective monomers. In the first report of the series,<sup>23</sup> cerium oxide (CeO<sub>2</sub>) and hematite ( $\alpha$ -Fe<sub>2</sub>O<sub>3</sub>) of different kinds viz. polyhedral (65 nm), spindle type (300 nm long), and silica-coated hematite, were prepared and desirably modified for use in this purpose. As synthesized particles or those treated with HCl were almost equally capable of initiating polymerization. But purified hematite particles, free from acidic adherence, and pure SiO<sub>2</sub> particles, both failed to synthesize nanocomposite colloid. This observation indicates that the active sites on the inorganic particles were the actual initiators for polymerization. IEP of the coated particles were almost identical to that of the bare particles, which implies that the surface of composite particles retain the properties of the core materials to some extent. CuO (1.6  $\mu$ m) in aqueous solution was chosen as the supporting material in another report<sup>24</sup> and a PAN-coated CuO composite was synthesized in an analogous technique in the presence of a stabilizer poly(vinyl alcohol) (PVA). Huang et al.<sup>25</sup> have reported identical studies using a variety of metal oxide particles of different sizes viz. CuO (1.6  $\mu$ m), CeO<sub>2</sub> (0.52  $\mu$ m),  $\alpha$ -Fe<sub>2</sub>O<sub>3</sub> (0.53  $\mu$ m), NiO (3.8  $\mu$ m), and spherical SiO<sub>2</sub> (0.46  $\mu$ m) as core materials where the aerial oxygen has been mentioned as an effective oxidant. In general, coating thickness and fraction of conducting polymer in composites were found to be controlled by the experimental parameters viz. concentration of monomer, reaction temperature, PVA concentration, presence of oxygen, etc. However, owing to the harshness of reaction conditions, higher temperature, and some other added effects, electrical conductivity of the resulting nanocomposites was immeasurably low in all cases. Very recently colloidal MnO<sub>2</sub> (10–20 nm) has been used by Biswas et al.<sup>26</sup> to synthesize stable PNVC-MnO<sub>2</sub> colloid.

A novel method of synthesizing colloidal PAN particles with BaSO<sub>4</sub> core was introduced by Gan et al.<sup>27</sup> following the inverse microemulsion route. Two microemulsions, stabilized by a nonionic oligo(ethylene oxide)-based emulsifier, were prepared containing aniline in BaCl<sub>2</sub> and APS in H<sub>2</sub>SO<sub>4</sub>, respectively. Upon mixing of these two, BaSO<sub>4</sub> particles (20 nm) were immediately formed followed by in situ polymerization of aniline on the BaSO<sub>4</sub> support. This resulted in formation of a nanocomposite with core-shell type morphology apparently in the form of a stable green dispersion. In another brilliant approach,<sup>28,29</sup> PPy-coated gold nanoparticles were synthesized within the microdomain of a diblock copolymer, providing an excellent means of formation of such dispersions. Diblock copolymers, owing to their ability to form microdomains and to associate in solution in the form of micelles, can provide small compartments inside which particles of a finite size can be generated and stabilized. Polystyrene-*block*-poly(2-vinylpyridine) (PS-*b*-P2VP), taken in toluene solution (0.5 mass %) was treated with tetrachloroauric acid (0.5 and 0.7 equivalent to 2VP units) which got selectively bound within the P2VP cores of the micelles. This solution was treated with pyrrole so that it diffused into the core of the micelles where polymerization was readily effected by HAuCl<sub>4</sub>, with simultaneous generation of Au nanoparticles and an in-situ formation of Au-PPy nanocom-

## Scheme 2. Formation of PPy-Au Nanocomposite in the Presence of Polymeric Micelles



posite (Scheme 2). The diblock supplied the core within which the composite was formed and stabilization could thereby take place. Formation of ultrafine Au nanoparticles (7–9 nm), surrounded by the shell of PPy (24 nm) within the core of micelle of the PS-*b*-P2VP copolymer, was confirmed from the TEM pictures.

In another excellent technique, PPy-(colloidal) gold nanocomposites have recently been introduced by Marinakos et al.<sup>30</sup> Although the work starts with template-guided polymerization, but ultimately provides template-free nanocomposite (particles, tubes, or wires). Au nanoparticles were arranged within the pores of an Al<sub>2</sub>O<sub>3</sub> membrane using a vacuum filtration technique. Afterward, Fe(ClO<sub>4</sub>)<sub>3</sub> was flown downward through the membranes which encounters rising pyrrole vapor within the membrane; PPy is grown within the pores of the respective film supporting the Au particles and the Au-PPy composite grown inside. After that the template membrane was slowly dissolved using 0.5 M KOH to set the composite particles free in solution. Excellent TEM pictures of the organized clusters of the present nanocomposites were collected (Figure 2), which reveal that the Au colloidal particles are located inside the PPy matrix and acting as nucleation sites for polymer growth.

**2. Nanocomposites with Improved Physical, Mechanical, and Electrical Properties.** Primarily the objective behind nanocomposite synthesis was to keep the conducting polymer in solution/dispersion and this stream of investigation is still alive. Later on, scientists became interested in other aspects of the nanocomposites viz. the thermal and electrical properties and versatile applications. Therefore, successful combination of different properties of the core materials viz. the magnetic, catalytic, electronic and optical properties, etc., with the existing properties of conducting polymers became the goal of scientists. Improvements in different physical properties of conducting polymers were also the subject of interest in this series of works. The present authors<sup>31,32</sup> have reported the synthesis of two PPy-based nanocomposites in which colloidal ZrO<sub>2</sub> (20–30 nm) and Fe<sub>2</sub>O<sub>3</sub> (25–50 nm) particles were incorporated into the PPy matrix by a simple chemical polymerization technique using FeCl<sub>3</sub> as oxidant. Macroscopic precipitation was observed although the incorporation of the inorganic component was confirmed from the TEM picture (Figure 3). In both these composites, the flakes such as nature of PPy changed and distinctly shaped

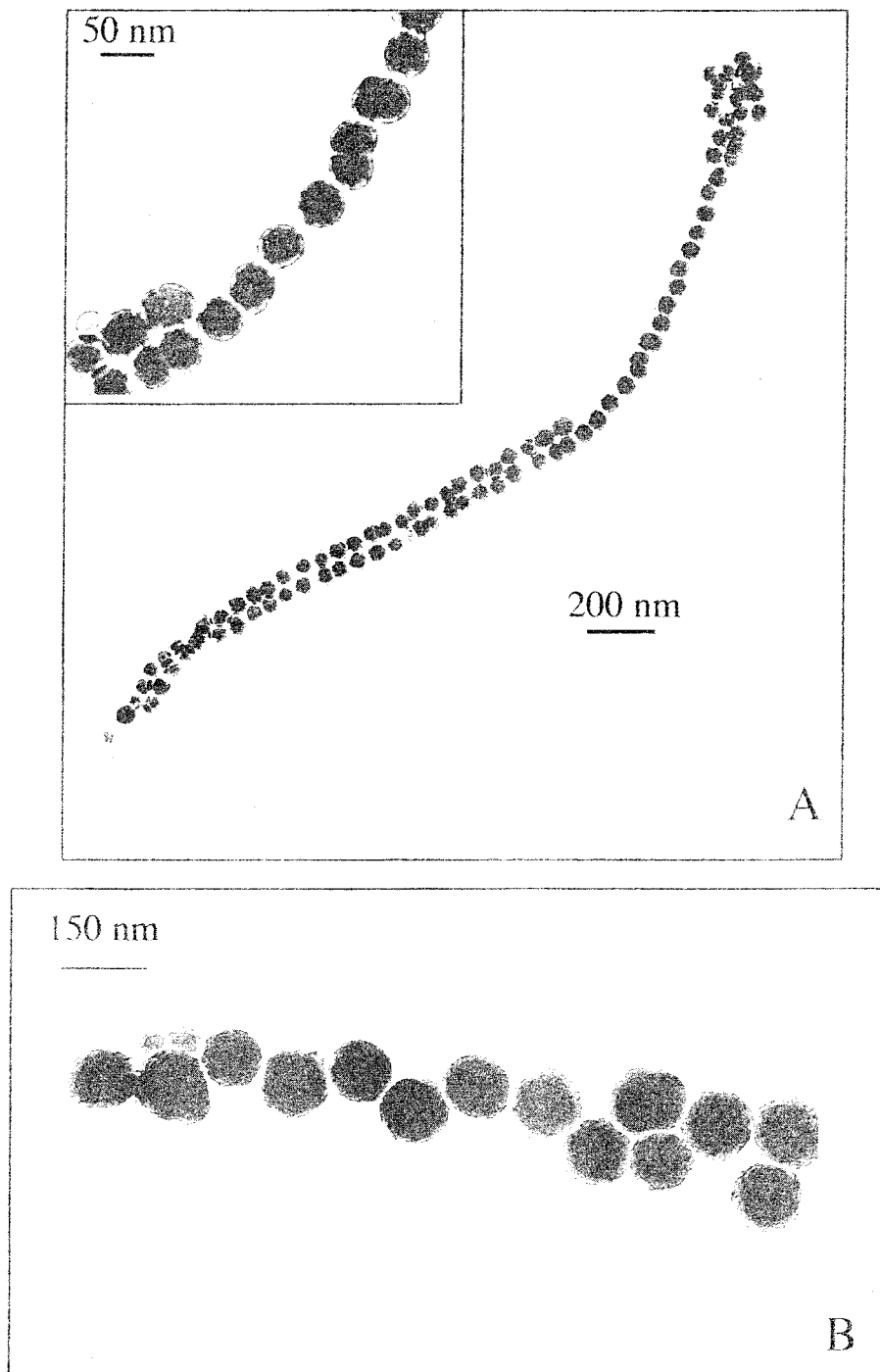


**Figure 2.** Transmission electron micrographs of 1D interconnected arrays of polypyrrole colloids. Polymerization using  $\text{Al}_2\text{O}_3$  membranes with (A) 20 nm and (B) 200 nm pore diameter. (Reproduced with permission from ref 30. Copyright 1998 American Chemical Society.)

particles were formed, resulting in some improvement in the compactness of the polymer as well as in the ordering of composite particles in their pressed pellets. Interestingly, despite insertion of insulating materials, the room-temperature dc conductivity of these two composites increased to a large extent (from  $\sim 1$  to  $\sim 17$  S/cm in PPy- $\text{ZrO}_2$  and from 20 to 90 S/cm in PPy- $\text{Fe}_2\text{O}_3$ ) on composite formation. The insulating particles being completely encapsulated in the conducting matrix, resistive interlinks do not form within the system. The increase in dc conductivity was thought to be a direct consequence of improved compactness of the polymer, as a result of which the coupling among the composite

particles through the grain boundaries improved which explains the reduced resistivity of the samples. In the PPy- $\text{Fe}_2\text{O}_3$  system, thermal and environmental stability of the polymer was also found to improve after composite formation. Recently Ray et al.<sup>33</sup> have combined poly(*N*-vinyl carbazole) (PNVC), a photoconducting polymer, with  $\text{SiO}_2$  to form another nanocomposite. In the presence of a polymeric stabilizer PVP, the resulting nanocomposite can be redispersed in water to form a stable suspension but in the absence of PVP, the dispersion is stable only up to 20 h.

Poly(*p*-phenylenevinylene) (PPV) is a well-known conducting polymer with excellent photoluminescence

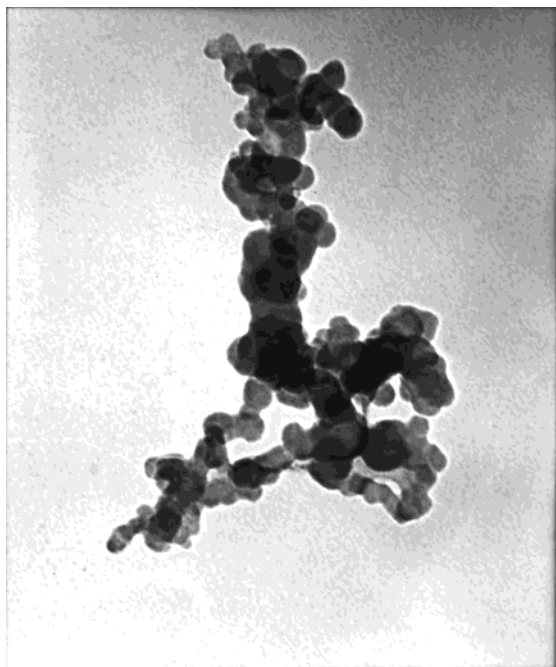


**Figure 3.** Transmission electron micrographs obtained from nanocomposite with lowest PPy loading. (Reproduced from ref 32. Copyright 1999 Elsevier.)

(PL) properties. However, modulation of different physical properties of PPV by incorporating nanosized  $\text{TiO}_2$  particles (n- $\text{TiO}_2$ ) into it has been reported for the first time by Baraton et al.<sup>34</sup> PPV solution and n- $\text{TiO}_2$  (21 nm and BET surface area  $50 \text{ m}^2/\text{g}$ ) in  $\text{CHCl}_3$  were mixed in several mass ratios under stirring and ultrasonication to obtain the nanocomposite solution/dispersion. Promising oxygen sensing properties have been demonstrated by this nanocomposite through a reversible PL emission intensity modulation by oxygen adsorption. Very recently Hori et al.<sup>35</sup> have reported a novel technique for obtaining a three-component conducting film in which PAN and a metal oxide was entrapped into a silica matrix by sol-gel method. Water-soluble PAN was prepared by doping with dodecylbenzene sulfonic acid (DBSA). This was mixed with phenyltriethoxy silane (PTES), ethanol, water, and the metal oxide particles viz.  $\text{TiO}_2$  ( $\sim 10 \mu\text{m}$ ),  $\text{Al}_2\text{O}_3$  (35–50  $\mu\text{m}$ ),  $\text{MgO}$  (2–4  $\mu\text{m}$ ), etc. upon stirring. In almost all cases, conductivity falls on mixing with insulating metal oxide particles while thermal stability of PAN was improved. Unlike pure PAN, conductivity of the metal oxide-entrapped PAN increased up to  $\sim 100^\circ\text{C}$ .

Carbon black (CB)-filled composites have a very long history especially in the field of plastics and rubber industries. However, the idea of utilizing this conducting particle as core material of conducting nanocomposites was brought about by Wampler et al.<sup>36a,b</sup> In this novel work CB not only serves as the inorganic core but also helps in doping, due to the acid groups present in it. Simple  $\text{K}_2\text{S}_2\text{O}_8$  initiated chemical polymerization of pyrrole in the presence of CB completed the formation of nanocomposite. At a very low level of incorporation, CB itself cannot form a conducting channel but disrupts the interchain electronic conduction of PPy itself; therefore, at that level, CB loading results in decreasing dc conductivity of PPy. After a critical CB loading, the classical percolation behavior is observed with these

composites, showing a saturation at 60% CB. Surface area calculations have differentiated the CB-PPy composites from the respective physical mixtures; but above a loading level of  $\geq 43\%$ , there is a surplus of CB and the CB character predominates in the composites. PPy-CB composites are large surface area materials, retaining the properties of the components. The compacted powder of these composites has shown their efficiency toward reduction of Cr(VI) to Cr(III) and the composites have outperformed both the polymer and CB in its reducing property.

Very few examples are available regarding the mechanism of electrical transport in the nanocomposites. In the CB-PPy composite,<sup>36a</sup> low-temperature (15–300K) dc conductivity studies have been performed which revealed that neither of the models, variable range hopping (VRH) or thermal fluctuation-induced tunneling of carriers (TFTC), works very well with these solids. Composites with higher CB loading ( $\geq 43\%$ ) barely shows any temperature gradient of conductivity and are of least importance in this purpose. Very recently we<sup>37</sup> studied this phenomenon in detail through the measurements of temperature-dependent dc ( $\sigma_{dc}$ ) and ac conductivity ( $\sigma_{ac}$ ) and thermoelectric power (TEP) with a series of PPy- $\text{Fe}_2\text{O}_3$  nanocomposites.  $\sigma_{dc}$  data satisfactorily fit the VRH model while a complex behavior is shown by the TEP values. In lower temperature region ( $\leq 225 \text{ K}$ ), TEP varied linearly with temperature, showing a metal like behavior but deviates from linearity at higher temperatures (Figure 4).  $\sigma_{ac}$  also showed some nonconventional behavior; it was almost unchanged up to a critical frequency followed by a jump and a continuous increase (Figure 5). This result could not be explained by any single existing theory and a heterogeneous model was proposed in which highly conducting islands were connected with poorly conducting barriers in a complicated fashion.

**3. Nanocomposites with Magnetic Susceptibility.** Over past few years, there has been a great deal of attention about the attractive magnetic behavior of PAN and PPy. In parallel with the synthesis of conducting polymers in their respective magnetic forms, integration of magnetic nanoparticles with conducting polymers has become an area of particular interest. An overall assessment of the efforts in producing nanostructured conducting polymer composites and nanocomposites has been done by Kryszewski et al.<sup>38</sup> in a short review. Successful combination of magnetic susceptibility with electrical conductivity was first reported by Butterworth et al.,<sup>39,40</sup> who succeeded in synthesizing a PPy-based nanocomposite in a conventional chemical polymerization method with silica-coated magnetic (MS) particles (5–30 nm) as the core material. These ultrafine particles, prepared in a technique followed by Philips et al.,<sup>41</sup> were expected to combine the unique dispersing ability of normal  $\text{SiO}_2$  particles with magnetic susceptibility of hematite. The resulting composite was inferior to the pure polymer in electrical conductivity ( $10^{-3} \text{ S/cm}$ ) and showed superparamagnetic behavior with an appreciable magnetic susceptibility of 6.5 emu/g, less than that of the pure colloid (23 emu/g). Higher silica loading yielded more stable dispersion with reduced conductivity and bulk magnetization. In another contemporary publication a superparamagnetic  $\gamma\text{-Fe}_2\text{O}_3$ <sup>42</sup> particle (9 nm)

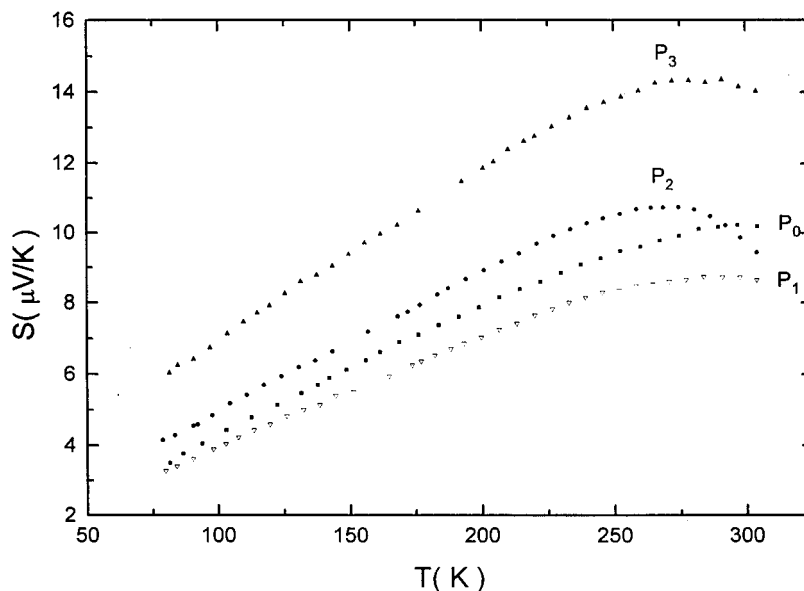


**Figure 4.** Variation in TEP ( $S$ ) with temperature ( $T$ ) for PPy- $\text{Fe}_2\text{O}_3$  nanocomposites.  $P_0$  presents pure PPy and  $P_1$ ,  $P_2$ ,  $P_3$  present nanocomposites. (Reproduced from ref 37. Copyright 1999 American Institute of Physics.)

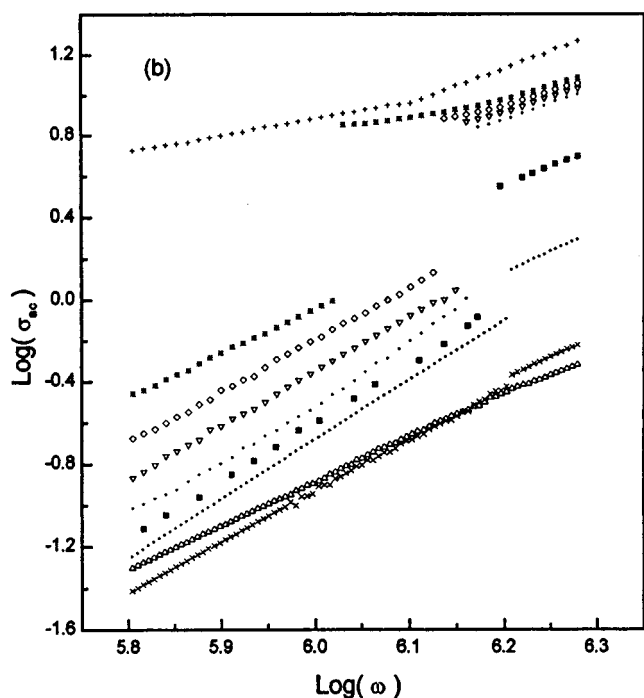


**Figure 5.** Variation in logarithmic  $\sigma_{ac}$  as a function of logarithmic frequency ( $\omega$ ) for PPy- $\text{Fe}_2\text{O}_3$  nanocomposite at different temperatures (From top:  $T(K) = 250, 220, 190, 160, 130, 100, 70, 45, 14$ ). (Reproduced from ref 37. Copyright 1999 American Institute of Physics.)

included composite was prepared by polymerizing pyrrole-*N*-propylsulfonate with  $\text{FeCl}_3$  and subsequently treating the material with  $\text{NH}_4\text{OH}$  at  $70^\circ\text{C}$ . An almost similar work was published by Wan et al.,<sup>43</sup> who synthesized a nanocrystalline  $\text{Fe}_x\text{O}_y$  (14 nm) incorporated PAN nanocomposite by mixing an aqueous solution of  $\text{FeSO}_4$  (5.9%) with a 1.6% solution of PAN (emeraldine base form, EB) in *N*-methylpyrrolidone (NMP) under an  $\text{N}_2$  atmosphere. Color and conductivity of the nanocomposite was dependent on the pH of reaction medium. In an acidic medium (pH 1.0), a green colored precipitate, having no magnetic susceptibility was obtained ( $\sigma = 10^{-4}$  S/cm). In neutral (pH 7.0) or

alkaline (pH 14.0) medium, a black precipitate appeared with poorer conductivity and stronger magnetic susceptibility in the latter case. Binding energy calculations reveal that iron oxide incorporated into the PAN matrix at alkaline pH was nanocrystalline  $\text{Fe}_3\text{O}_4$  which contributes to the observed super-paramagnetic behavior of the composite. In a modified technique,<sup>44</sup> the nanocomposite was obtained by adding a mixture of  $\text{FeCl}_2 \cdot 4\text{H}_2\text{O}$  and  $\text{FeCl}_3 \cdot 6\text{H}_2\text{O}$  followed by the addition of a designated concentration of aqueous KOH solution. The ultimate composite possesses both electrical conductivity and magnetic susceptibility, controlled by the concentration of KOH. By increasing the percentage of KOH used, the  $\text{Fe}_3\text{O}_4$  content as well as magnetization can be increased up to a level while the conductivity falls off. By using a water-soluble copolymer poly(aniline-*co*-aminobenzenesulfonic acid) (PAOABSA), an easier technique of synthesizing a nanocomposite with ferromagnetic properties has been reported by the same group of authors.<sup>45</sup> However, these two contemporary works differ from each other in the point that the ferromagnetic particle is  $\gamma\text{-Fe}_2\text{O}_3$  in the latter, as compared to  $\text{Fe}_3\text{O}_4$  in the former.

An elegant method for synthesizing a superparamagnetic nanocomposite film with appreciable electrical conductivity using chemical polymerization technique, has recently been reported by Tang et al.<sup>46</sup> Ultrafine  $\gamma\text{-Fe}_2\text{O}_3$  particles (10 nm) were first coated with anionic surfactants viz.  $\omega$ -methoxy-poly(ethylene glycol) phosphate (PEOPA) and dodecylbenzenesulfonic acid (DBSA) to prevent the aggregation of the particles as well as to enhance their miscibility with PAN solution. Afterward, the dispersion of the coated magnetic particles (in NMP) were mixed with solutions of PAN-PEOPA, PAN-DBSA, and PAN-CSA, using NMP, chloroform, and *m*-cresol as common solvents which were subsequently film casted to produce free-standing films of  $\gamma\text{-Fe}_2\text{O}_3$  containing PAN. Conductivity of highly conducting (237 S/cm) pure PAN-CSA film was lowered on addition of  $\gamma\text{-Fe}_2\text{O}_3$ -DBSA, although the ultimate values obtained were much higher (180 and 82 S/cm with 20.8% and 47.5%



$\gamma$ -Fe<sub>2</sub>O<sub>3</sub>, respectively) than that so far reported. The  $\gamma$ -Fe<sub>2</sub>O<sub>3</sub>-DBSA/PAn-CSA film was found to possess appreciable magnetic susceptibility and saturation magnetization at 25 emu/g  $\gamma$ -Fe<sub>2</sub>O<sub>3</sub> (300 K) and 40 emu/g  $\gamma$ -Fe<sub>2</sub>O<sub>3</sub> (5 K), respectively. A very important report has recently been published<sup>47</sup> with regard to the effects of the structure of two different nanosized materials on the properties of the resulting composites. V<sub>2</sub>O<sub>5</sub> and Fe<sub>3</sub>O<sub>4</sub>, having layered and close packed structures, respectively, were combined with PAn using chemical polymerization technique and two different charge-transfer phenomena were revealed. In the V<sub>2</sub>O<sub>5</sub>-PAn system, V<sup>5+</sup> ions directly interact with PAn macromolecules while some amount of surface charge carried by the Fe<sub>3</sub>O<sub>4</sub> particles is transferred to the PAn in PAn-Fe<sub>3</sub>O<sub>4</sub> system by which Fe<sub>3</sub>O<sub>4</sub> particles serve an extra dopant to PAn.

**4. Nanocomposites with Dielectric Property, Energy Storage, and Catalytic Activity.** After the discovery of interesting dielectric properties of conducting polyacetylene, a lot of works have been carried out in this respect with different conducting polymers. Dielectric property of nanocomposites was first studied by Mujauchi et al.<sup>48</sup> using a barium-titanate (BT)-PPy nanocomposite. The fraction (%) of PPy was very low (0.3–1.4) in these nanocomposites, which resulted in a low dc conductivity (0.01 S/cm) compared to pure PPy (10<sup>3</sup> S/cm) and other nanocomposites. However, the most important observation was that the relative permittivities ( $\epsilon_r'$ ) of the composites, measured at the range of 100 Hz to 1 MHz, have a higher value than both PPy and pure BT. Owing to the presence of PPy, the composites possess higher  $\epsilon_r'$  than BT but the comparison with PPy was not well explained. Recently two reports<sup>49a,b</sup> have been published in which the same group of scientists have combined BT and TiO<sub>2</sub> (100 nm) with PAn to produce two different piezoresistive composites. Both the nanoparticles were synthesized in the sol-gel method and the simple chemical polymerization technique was followed for composite formation. Pressed pellets of the composites were subjected to I-V measurements which revealed that electrical transport as well as observed piezoresistivity in such composites are governed by the space charge limited conduction (SCLC) process.

The heteropolyanions viz. the phosphomolybdates (PMo12) and polyonometalates (POM) have drawn a great deal of attention from the point of view of their structural, spectroscopic, and catalytic properties. However, only recently have they been combined with the conducting polymers so that their material aspects can be explored. Romero et al.<sup>50</sup> have tried to incorporate the phosphomolybdate anions into polyaniline matrix as dopants with the aim of building a useful cation insertion electrode. The synthesis of the hybrid material PAn/PMo12 was carried out in two steps. In both, in the chemical synthesis route, aniline was directly added to solid phosphomolybdic acid (H<sub>3</sub>PMo<sub>12</sub>O<sub>40</sub>), resulting in formation of a black precipitate and a deep blue solution and finally to a black-green powdery solid. This powder was used as a starting material in the electrochemical synthesis technique. It was dissolved in water and a thin film of hybrid material was obtained on the electrode by repeated potential cycling of the solution.

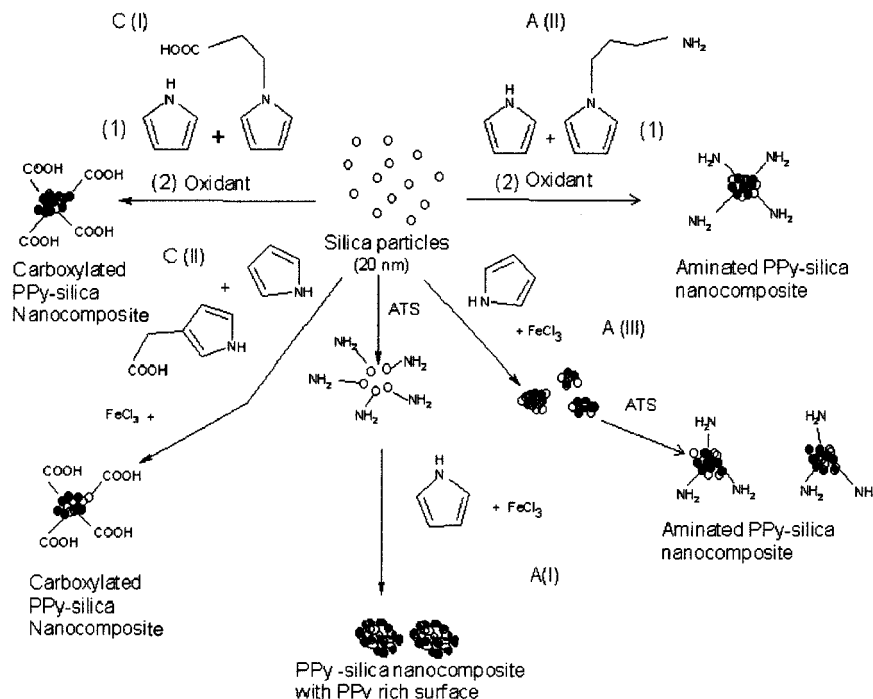
The same powder was stirred in water for a long period of 24 h with bubbling of oxygen to obtain a black precipitate of chemically synthesized hybrid material. Relevant electrochemical analyses have proven that the PMo12 cluster anion is an integral part of the hybrid material, anchored firmly in the polymer matrix, acting as an oxidizing agent and at the same time as an acid and dopant. Because of its high charge and large size, the anion is reluctant to be released from the material. Anchoring of PMo12 leads to the insertion and deinsertion of cations for charge compensation during reduction and oxidation which presents an important modification in the cycling mechanism of polymeric electrodes.

Unique redox properties of PAn, PPy, and other conductive polymers have lured scientists to utilize them as cathodic materials in rechargeable Li battery. But the poor charge discharge capacity of them has hampered their successful application in this respect. The maximum amount of electrolyte anion that can be incorporated into oxidized films of PPy and PAn is only 0.3 and 0.5 mol per mole monomer unit, respectively. This limitation could be overcome to some extent by incorporating cathode active materials into ICP matrix. For this context LiMn<sub>2</sub>O<sub>4</sub> and crystalline V<sub>2</sub>O<sub>5</sub> has been embedded into PPy<sup>51</sup> and PAn<sup>52</sup> respectively. In a solution of reduced state of PAn (blue) in NMP, V<sub>2</sub>O<sub>5</sub> particles were well dispersed and a composite film was cast on the electrode. Charge-discharge analyses proved that a 96:4 ratio of V<sub>2</sub>O<sub>5</sub> and PAn presents the optimum composition for the system to act as a high energy density electrode material. Here PPy and PAn not only serve the conductive binder like carbon powder in batteries, but also participate as active materials.

Conducting polymers have been used as the supporting matrix in different composites for intercalation of catalytically important nanoparticles so that the catalytic activity can be retained in the composite. A few such hybrid materials have been synthesized by Qi and Pickup, who have incorporated Pt<sup>53,54</sup> and PtO<sub>2</sub><sup>55</sup> in a matrix of PPy and a polyanion poly(styrene sulfonate) (PSS). In these nanocomposites oxygen reduction properties of the nanoparticles were prevailing while electrical conductivity suffered remarkably. This difficulty was successfully overcome to a large extent by using poly(3,4-ethylenedioxythiophene) (PEDOT) as the conducting polymer component. In this work EDOT was polymerized in the presence of aqueous NaPSS solution and the resultant composite (conductivity 9.9 S/cm) was stirred in aqueous formaldehyde (18%) solution of H<sub>2</sub>-PtCl<sub>6</sub>·xH<sub>2</sub>O to deposit Pt nanoparticles (~4 nm) on the composite particles. This treatment resulted in a lowering of the conductivity of the catalyzed material to 4 S/cm. The hybrid material works well as electrode of fuel cell and its performance is comparable to the commercial carbon supported catalyst at a higher Pt loadings.

PPy and PAn have the ability to reduce and precipitate some of the metals from their respective acid solutions. On the other hand PPy-SiO<sub>2</sub> and PAn-SiO<sub>2</sub> hybrid nanocomposites, as discussed earlier, offer the advantage of a material with large surface area. These two important characteristics have enabled the above-mentioned nanocomposites to be an attractive host for entrapping a substantial amount of metal particles with

**Scheme 3. Different Techniques of Surface Functionalization of PPy-SiO<sub>2</sub> Nanocomposites by Amino Groups and Carboxyl Groups**



important catalytic activity and these metal-rich composites can be used for subsequent catalytic application, as postulated<sup>56a,b,57</sup> recently. Pure PAN and PPy with their composites PPy-SiO<sub>2</sub> and PAN-SiO<sub>2</sub> were prepared in doped forms and were subsequently reduced and dedoped to PAN (LM) and PPy (PPy<sup>0</sup>) and their nanocomposites. All these materials and pure SiO<sub>2</sub> were separately added to dilute aqueous solutions of HAuCl<sub>4</sub> (in HCl) and PdCl<sub>2</sub> (in HCl) of known concentration, under constant stirring. Reduced forms of the polymers were converted to the respective oxidized forms with simultaneous in situ reduction of metal ions Pd(II) and Au(III) to their elemental forms. Uptake of metal revealed that PPy<sup>0</sup> and LM were much more effective in this purpose as compared to the doped, oxidized forms. Nanocomposites have been proven to be better adsorbents of metals than the pure polymers. This result is a direct consequence of larger specific surface area of the composites compared to the polymers. However, the catalytic activity of Pd was retained; SiO<sub>2</sub>-PAN-Pd hybrid was capable of removing dissolved oxygen from water and fully converting nitrobenzene to aniline. Therefore, nanocomposite particles present a potentially useful material for recovery of precious metals as well as for important catalytic applications. Pd inclusion in PAN (emeraldine base) system has also been separately reported by Drelinkiewicz et al.<sup>58</sup> in an almost similar technique. The catalytic properties of Pd and Pd<sup>2+</sup> was retained on entrapment and the catalytic efficiency is higher with Pd(0) containing samples.

**5. Nanocomposites with Surface Functionalized Core and/or Shell.** Works done by Armes et al. utilizing different type of SiO<sub>2</sub> particles as colloidal support for conducting polymers have been discussed earlier. Despite the deep black color of the resulting colloid, surfaces of the composite colloid were found to be silica rich instead of PPy rich. Later on, porous silica gel was used by Wallace et al.<sup>59,60</sup> as a support material

for synthesis of PPy- and PAN-modified silica gel particles, the chromatographic properties of which were explored by HPLC. Silica particles were exposed to monomer solution prior to chemical oxidative polymerization in aqueous medium. The method has been repeated by Perruchot et al. and preliminary XPS data have proven that the surface of composite still remains silica rich. To improve the adhesion of PPy to the inorganic substrates which may, in turn, produce PPy-rich composite particles, the latter group has utilized silane chemistry to functionalize silica particles.<sup>61,62</sup> Different methodologies have been followed for introducing -NH<sub>2</sub> or -COOH functional groups into the PPy-SiO<sub>2</sub> nanocomposite particles which have been collectively presented in Scheme 3. Aminopropyl triethoxy silane (ATS) was utilized to add -NH<sub>2</sub> functional groups to the surfaces of silica and silica gel particles prior to the deposition of PPy on them. ATS was hydrolyzed in a water-ethanol mixture (1:9 v/v) and then a measured amount of silica gel was added to it and was stirred overnight to get the ATS Silica particles [A(I)]. These modified particles were subsequently treated with pyrrole which was then polymerized, resulting in the formation of PPy-coated composite particles. XPS studies performed on these materials have proven that ATS adsorption on silica surface was of Langmuir type. After ATS treatment, PPy loading in composites increases depending upon the ATS concentration and leads finally to a silica-ATS/PPy composite with a PPy-rich surface. This method of functionalizing the inorganic substrate with the aim of increasing PPy adherence was brought about by Faverolle et al.<sup>63,64</sup> who have deposited PPy as a thin and coherent layer (20–50 nm thick) on E-glass fiber (14 mm diameter). Glass fibers were pretreated with ATS and a pyrrole-functionalized silane coupling agent followed by the polymerization of pyrrole on them. The resulting composites revealed that the PPy coating was

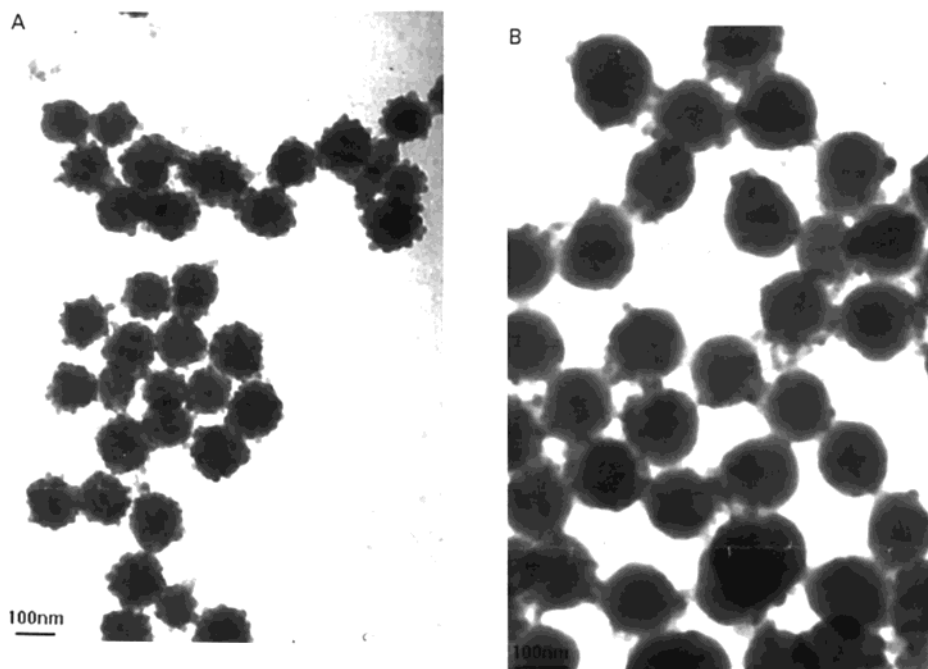


**Figure 6.** Representative transmission electron micrographs for aminated PPy-SiO<sub>2</sub> nanocomposite particles obtained from (A) ATS treatment and (B) Copolymerization. (Reproduced with permission from ref 72. Copyright 1998 Springer Verlag.)

discontinuous and less dense with untreated glass fibers while those obtained with the modified substrates led to a more regular, thick and homogeneous PPy overlayer. Moreover, silane coupling agents resulted in improving the adhesion between the as prepared conducting E-glass fibers and another insulating resin matrix when the latter was used as a reinforcing material.

The above-mentioned functionalizations, applied to the inorganic substrates can enhance the PPy loading in the composites which in turn improves the electrical conductivity and some other material properties of the same. But PPy colloids have another interesting application as marker particles in visual agglutination immuno-diagnostic assay of different hormones, antigens, and antibodies. The intense intrinsic coloration as well as narrow particle size distribution of PPy latex particles are the value-added properties in this respect. Now, PPy- and PPy-silica-based immunoreagents are made by coating the particles with specific binding ligands (e.g., any antigen or antibody); the efficiency of any such reagent can be improved if the contact can be made through an intervening spacer molecule rather than by simple adsorption. At the same time minimizing the nonspecific binding interactions should also be beneficial for applications of PPy colloid in such assay. Here comes the idea of functionalizing the surfaces of colloid particles with -NH<sub>2</sub> or -COOH groups. The amine functionalization was performed by J. Goodwin et al.<sup>65</sup> and A. Philipse et al.<sup>66</sup> just by adding composite particles to a stirred aqueous solution of ATS. This treatment [A(III)] provides an aminated surface to the nanocomposites, confirmed from their IEP at pH 7, equal to that obtained<sup>21a</sup> for aminated bare silica colloid. However, functionalization in this case occurs mainly on silica surface and the colloids suffered from a lower degree of amination and irreversible flocculation on prolonged storage. Carboxyl functionalized PPy-SiO<sub>2</sub> microparticles was primarily reported by Maeda et al.<sup>67</sup>;

polymerizing pyrrole and 1-(2-carboxyethyl pyrrole) by APS or FeCl<sub>3</sub>, in the presence of ultrafine silica (20 nm), they obtained the desired surface functionalized PPy-SiO<sub>2</sub> particles [C(I)] for diagnostic assay. Resulting composite particles were similar in properties to the functionalized PPy colloids reported by Tarcha et al.<sup>68</sup> A comparison was made<sup>69</sup> among the three materials, the PPy-PVA latex, PPy-COOH and PPy-COOH-silica microparticles in respect of the specific activity of an immobilized monoclonal antibody to human chorionic hormone (hCG). However, poor copolymerizability of gonadotropin N-substituted pyrrole with pyrrole led to poor robustness and nonreproducibility of the colloidal composite and the comparison revealed no added advantage of the surface functionalization. Later on, McCarthy et al.<sup>70</sup> synthesized carboxylated PPy-SiO<sub>2</sub> colloid of prolonged stability with pyrrole-3-acetic acid [C(II)] and using an H<sub>2</sub>O<sub>2</sub>-based oxidant system. The monomer, synthesized previously following an established technique was copolymerized with pyrrole in the presence of ultrafine silica sol. The resulting colloid proved itself as an excellent candidate for new marker particles in immuno-diagnostic assays. Moreover, the particles were much more efficient in DNA adsorption<sup>71</sup> compared to noncarboxylated one.

Goller et al.<sup>72</sup> have prepared the aminated PPy-silica composites in two different routes, one is silylation as reported by Goodwin et al.<sup>65</sup> and another is copolymerization technique similar to that followed for carboxy functionalization.<sup>67-70</sup> In the latter one pyrrole and 1-(3-aminopropyl)pyrrole were copolymerized by FeCl<sub>3</sub> in the presence of silica sol to obtain the nanocomposite particle with pendant -NH<sub>2</sub> groups [A(II)]. The TEM pictures of both of the sols bear very clear evidences of such surface amination [Figure 6.]. The  $\zeta$  potential vs pH curves of pure silica sol, surface aminated silica (after ATS treatment) and aminated PPy-SiO<sub>2</sub> nanoparticles have revealed that the last two curves are almost identical (s-shaped) which is more evidence in

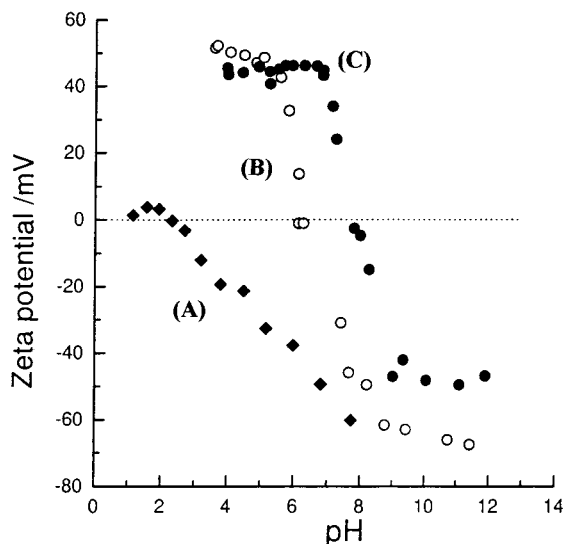


**Figure 7.**  $\zeta$  potential vs pH data for (A) silica sol (monosphere 250, ex. E. Marck); (B) the aminated silica sol obtained after ATS treatment; and (C) aminated polypyrrole-silica nanocomposite particles obtained after ATS treatment. (Reproduced with permission from ref 72. Copyright 1998. Springer Verlag.)

support of successful surface amination of the nanocomposite particles (Figure 7). However neither of these two techniques could prevent the macroscopic precipitation of the amino-functionalized sols within several weeks. Such poor shelf life presents them as unsuitable for diagnostic applications.

### III. Electrochemical Preparations

Electrochemical synthesis of conducting polymers is a well-established technique that can successfully incorporate a wide spectrum of electrolyte anions soluble in the polymerization medium, into the growing chain of conducting polymers viz. PPy and PAn. This is, in fact, an efficient tool for introducing different properties like electrocatalytic activity, magnetic property, etc. in the respective conducting polymers. At the same time electrochemistry has provided equally efficient techniques for incorporating insoluble particles of metal/metal oxide, etc. into growing polymer films, giving birth to a number of hybrid nanocomposites. This requires generation of surface negative charge on the respective particle, which is the key to success of such techniques and is achieved in different ways. Depending on the versatile properties and important application potential, these composites can also be classified into different categories as discussed here.

**1. Nanocomposites with Charge Storage and Electrochromic Activities.** In the pioneering work of this series Yoneyama et al.<sup>73</sup> could successfully attach  $\text{WO}_3$ ,  $\text{SiO}_2$ ,  $\text{SnO}_2$ , and  $\text{Ta}_2\text{O}_5$  particles into an electrochemically growing PPy film. In the original experiment, oxide particles were dispersed in the aqueous solution of pyrrole, the pH of which was kept above the IEP of the respective oxide so that negative charge is built on their surface. During the electrochemical growth the latter serves as the counteranion and is accordingly combined with the PPy film. On the other hand, pH of the medium should not be too high so as to inhibit polymer growth. Therefore, oxides with lower IEP, e.g.  $\text{WO}_3$  (0.54),  $\text{SiO}_2$  (1.8),  $\text{Ta}_2\text{O}_5$  (2.9), and  $\text{SnO}_2$  (4.5) could be included into PPy films in this manner while  $\text{TiO}_2$

(6–6.7),  $\text{CeO}_2$  (6.8),  $\text{MnO}_2$  (7.3), and  $\text{ZnO}$  (9.0) requiring pH  $\sim 8$ –10 did not incorporate at all. Oxide incorporation was evident from SEM pictures and XRD spectra as well as cyclic voltammograms obtained for oxide-rich PPy films. Another insoluble colloidal particle Prussian Blue (PB),  $\text{Fe}_4[\text{Fe}(\text{CN})_6]_3$ , has also been included into a PPy film as a dopant<sup>74</sup> following the same electrochemical deposition technique. In this case, the pH of the deposition bath containing pyrrole (0.1 M) and PB ( $2 \times 10^{-3}$  M) was kept 5.7, at which PB is negative and is capable of moving toward the anode to attach with the PPy film. When the pH was lowered to 2.5, the negative charge is lost and PPy film is not grown. During electrochemical characterization PB doped films exhibited two redox peaks, owing to two different Fe(III) sites, one is fully hexacoordinated by  $-\text{NC}$  ligand and another is partially hydrated. In a very recent publication, Ogura et al.<sup>75</sup> have reported a combined electrode in which PB is deposited on Pt substrate and is subsequently covered by PAn film. The whole system was used for catalytic  $\text{CO}_2$  reduction.

However, the aim of incorporating a spectrum of metal oxides was not left here. Later on it was discovered that the oxide particles as well as the deposition medium might be modified to perform successful incorporation of oxide particles into PPy. In a later publication, Kawai et al.<sup>76</sup> reported two such techniques. In one technique,  $\text{TiO}_2$  particles were negatively charged by the photoelectrochemical charging technique and are accordingly included in the PPy film as a conventional dopant anion during electrosynthesis. Another technique was to add a small amount of an electrolyte viz.  $\text{LiClO}_4$ ,  $\text{NaX}$  ( $\text{X} = \text{Cl}^-$ ,  $\text{Br}^-$ ,  $\text{I}^-$ ,  $\text{NO}_3^-$ ,  $\text{BF}_4^-$ ),  $\text{Na}_2\text{CO}_3$ , or  $\text{Na}_2\text{SO}_4$  in the deposition bath with the expectation that the respective anions are adsorbed on the  $\text{TiO}_2$  particles, giving rise to surface negative charge on them. Accordingly they become capable of serving as a dopant anion, especially in a pH comparable to the IEP of  $\text{TiO}_2$  (6–6.5). The former technique failed to form a stable PPy- $\text{TiO}_2$  film; although the negatively charged  $\text{TiO}_2$  particles were formed, only a very thin, resistive deposition of PPy was observed on the electrode. In the latter route, only  $\text{NaI}$  and  $\text{Na}_2\text{SO}_4$  succeeded in forming  $\text{TiO}_2$  incorporated thick and smooth PPy film, whereas all other salts resulted in PPy film formation (smooth or rough). Success of this technique raised the possibility of incorporation of almost any kind of oxide by judicious selection of a supporting electrolyte. But incorporation of the oxides, which can be easily embedded, viz.  $\text{WO}_3$ ,<sup>77</sup> is hampered by the presence of a supporting electrolyte like  $\text{LiClO}_4$  which can act as an efficient dopant. Competitive doping occurs and a less  $\text{WO}_3$ -rich PPy film was obtained from a deposition bath containing pyrrole,  $\text{WO}_3$ , and  $\text{LiClO}_4$  as compared to the previous one lacking  $\text{LiClO}_4$ . Increasing the concentration of the latter, results in decreasing the  $\text{WO}_3$  content in the film and the surface conductivity increased accordingly.  $\text{TiO}_2$  incorporation in PPy film has also been reported by Wang et al.<sup>78</sup> who have electrodeposited PPy on a microporous  $\text{TiO}_2$  film cast on an ITO-coated glass electrode from a concentrated colloidal solution. Effect of polymerization conditions has been studied through the measurement of I–V characteristics of  $\text{TiO}_2$ -PPy complex film. The film has been shown to be a highly

conducting system with good uniformity and efficient current injection property.

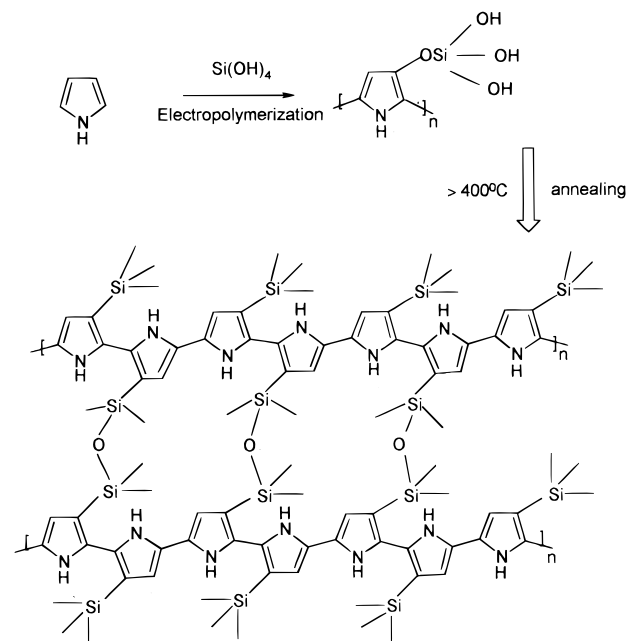
The improvement of charge–discharge capacity of conducting polymers by electrochemical incorporation of redox active materials has been performed by Yoneyama et al. Electropolymerizing pyrrole from a propylene carbonate (PC) solution containing tetraethylammonium chloride (TEACl) and as-prepared  $\beta$ -MnO<sub>2</sub><sup>79</sup> or Li–MnO<sub>2</sub><sup>80</sup> (0.3–0.6  $\mu$ m) the respective composites were formed. Li–MnO<sub>2</sub>/PPy was proven to possess larger capacity than  $\beta$ -MnO<sub>2</sub>/PPy, although the former was included in a smaller amount.

CB-incorporated PPy-based composites present another important class of materials with enhanced charge density and electrical conductivity. Such composites have been electrochemically developed first<sup>81</sup> by polymerizing pyrrole from a PC medium in the presence of LiClO<sub>4</sub> and CB. Later on Wampler et al.<sup>82a,b</sup> thoroughly studied the system for a range of CB concentrations (0.5–50 g/L). It was observed that CB content in the composites increased with increasing CB in medium. The amount of deposited material is almost trace and it requires large electrode area (10.5 cm<sup>2</sup>) to generate even milligram amounts of composite. In these composites CB acts as an effective surface modifier. Charge density of the thin and uneven composite film increased monotonically on increasing CB loading. At a highly negative potential (–0.8 V) at which PPy is essentially insulating, increased CB loading enhances the current density of composite, which suggests that CB–PPy is a better conductor than PPy itself. Like the chemically synthesized CB–PPy composites, the electrochemically grown thin film has also been employed for reduction of Cr(VI) by Wei et al.<sup>83</sup>

Ferric oxide nanoparticles are well-known for their photovoltaic properties which have turned them effective materials for solar energy storage. Zhang et al.<sup>84</sup> have electrochemically introduced these particles, of size 4 and 40 nm, into PPy film (grown from a CH<sub>2</sub>Cl<sub>2</sub> solution containing pyrrole and Bu<sub>4</sub>NClO<sub>4</sub>) by a spin-casting method between the growth period of two polymer layers. Considerable modification in electrochemical and optoelectronic behavior was observed, evident from surface photovoltage spectroscopic (SPS) responses.

Both PAN and WO<sub>3</sub> are two widely studied electrochromic materials of two different origins exhibiting color changes in two different potential ranges. PAN changes color from pale green to violet at anodic potentials 0.2–1.0 V (vs SCE), while WO<sub>3</sub> shifts from transparent to dark blue at cathodic potentials more negative than –0.1 V. Therefore, a successful combination of these two materials offers a transparent window between blue (WO<sub>3</sub>) and green (PAN) colors. Co-deposition of both components results in intimate mixing of the two, leading ultimately to a nonuniform color at any potential within this range. To avoid this difficulty Shen et al.<sup>85</sup> have synthesized a multilayer WO<sub>3</sub>/PAN composite with alternating layers of PAN and WO<sub>3</sub>. From a solution of aniline (0.1 M) and tungsten (0.25 M) in 0.25 M H<sub>2</sub>SO<sub>4</sub>, the composite was developed using a double potential pulse technique and the interwoven alternating layers were deposited by varying potential pulse. A dark blue WO<sub>3</sub> color at cathodic potential and violet

#### Scheme 4. Schematic Diagram of the IPN System Formed from Annealing of the Silanol-Functionalized Polypyrrole



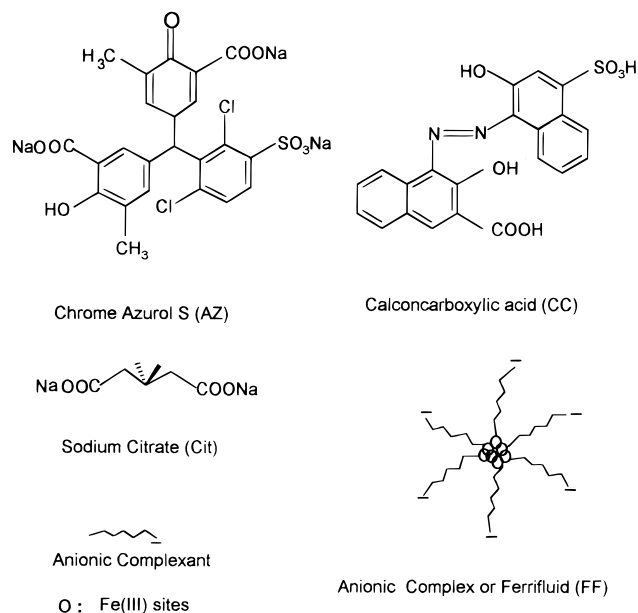
green multicolor at anodic potential was observed which is the key to the success of this composite as an effective electrochromic material.

A brilliant approach toward synthesizing a PPy-SiO<sub>2</sub> hybrid composite material has recently been reported by Komaba and Osaka.<sup>86</sup> They have electro synthesized PPy film in the presence of silanol; the latter is supposed to functionalize PPy by some chemical or electrochemical interaction during electropolymerization which guided the formation of a PPy-silanol composite film on electrode. Annealing the film at 400 °C for 1 h in a vacuum led to dehydration and subsequent condensation of silanol units, resulting in formation of a silica network around PPy chains. Therefore, the present composite material should better be termed as PPy-SiO<sub>2</sub> interpenetrating network (IPN) rather than PPy-SiO<sub>2</sub> nanocomposite (Scheme 4). The hybrid IPN was proven to be an efficient hole-transporting layer in electroluminescent (EL) devices.

Only a single report<sup>87</sup> so far has been published describing the synthesis and characterization of optically active PAN-silica nanocomposite using colloidal silica as the dispersant. At the same time this is the only example of electrosynthesis of nanocomposite in stable colloidal form. Aniline was polymerized in a three-electrode flow-through electrochemical cell using a solution consisting of colloidal silica (20 nm) and camphorsulfonic acid (HCSA) in optically active (1*S*, +) and (1*R*, –) forms. Stable optically active PAN colloid having particles 300–600 nm could be readily prepared, and raspberry morphology and the core–shell nature of which were revealed from TEM.

**2. Nanocomposites with Catalytic Properties.** The catalytic system for electrooxidation principally requires an efficient reversible redox process of the catalyst. At the same time some of the fuel cells operate in a strongly acid medium, which requires both the catalyst particles and their supports to be highly stable, for building a successful electrode. Therefore, appropri-

### Scheme 5. Structures of Anionic Complexants and Schematic Presentation of the Ferrifluid



ate particles dispersed in conducting polymers present a promising material for electrocatalytic applications. Catalytic particles dispersed along the entire thickness of the electrode leads to poor utilization of the catalyst. Therefore, conducting polymer bed with catalyst particles gathering near the surface presents an optimum situation in this respect. This principle has been followed in a good number of works describing the preparation of nanocomposites in which nanoparticles of Pt, Pd, Cu, etc. are combined with PPy, PAn, and PTH. Dispersion of Pt particles in PAn matrix and their ability for methanol oxidation was earlier described.<sup>88,89</sup> Formation of bimetallic electrodes by deposition of two metals at a time was first reported by Swathirajan et al.<sup>90</sup> On a poly(3-methyl thiophene) (P3MT)-modified electrode they have electrodeposited Pt and Sn from aqueous solutions (pH 1.7) of chloroplatinic acid and SnCl<sub>2</sub>. Recently Athawale et al.<sup>91</sup> have described the formation of a series of such monometallic and bimetallic electrodes in which Pd, Cu, Pd/Cu, and Cu/Pd have been combined with PAn in a method similar to Swathirajan et al. Successful oxidation of formic acid and methanol has also been reported there. In another communication,<sup>92</sup> microparticles of Cu and Pd have been deposited on PPy- and P3MT-modified Pt electrodes by electrodeposition from CuCl<sub>2</sub> and PdCl<sub>2</sub> solutions. Electrical resistance of these samples significantly changes in the presence of different gases at various concentrations and, therefore, presents themselves as promising materials for gas-sensing applications.

**3. Nanocomposites with Magnetic Susceptibility.** The novel method of electrochemical insertion of specially designed magnetic particles into growing PPy chain was first reported by Bidan et al.<sup>93a,b</sup> The "tailor-made" magnetic particles used in this purpose were in fact macroanions in which  $\gamma$ -Fe<sub>2</sub>O<sub>3</sub> is surrounded by an anionic complexing shell (Scheme 5). Three specific complexing agents have been chosen by the authors namely the sodium citrate, chrome azurol S (AZ), and calconcarboxylic acid (CC). Magnetic fluid or ferrofluid (FF) is formed by suspending these magnetic anions

(0.5–1  $\mu$ m) in an organic solvent stabilized by a surfactant, or an ionic stabilizer. When pyrrole is electropolymerized in the presence of the FF in absence of any other support electrolyte, the magnetic macroanions are incorporated in the growing PPy chain as a classical anion. For the resulting PPy-FF/Cit, the magnetic moment of a microdomain is much bigger than that for a single molecule; particles of this kind are said to be superparamagnetic. Further studies on magnetization measurements<sup>94</sup> and Mossbauer spectroscopic investigations<sup>95</sup> on these materials revealed that  $\gamma$ -Fe<sub>2</sub>O<sub>3</sub> particles are equally included into the PPy matrix, irrespective of their size, and they are fairly distributed in the polymer film (100  $\mu$ m thick) without formation of aggregates or without growing any major interactions within themselves. Neither the magnetic property of the particles is hampered on inclusion in the film, nor do they hamper the electrical conductivity of the polymer, which is a very good observation with respect to the application potentials of these composites.

### IV. Conclusion

Conducting polymer nanocomposites are very important inclusions in the list of novel materials and composites although their history is not older than 10 years. From the point of versatility of synthesis techniques, properties, and broadness of the scope of application, these materials have raised a great deal of scientific and technological interest and have led the research in materials science in a new direction. The present review provides an up to date account of the various approaches toward the synthesis and characterizations of these materials. Progress made in this respect are in fact successful strides toward the improvement of the processability and application potential of the respective conducting polymers in order to present them as materials suitable for versatile practical applications, some of which are discussed in proper context. By varying the nature of the component materials and the reaction parameters, some of the physical properties namely colloidal stability, magnetic susceptibility, electrochromic property, etc. have been improved which was not possible by a simple mixture or blending. However, the total control over the system is yet achieved and materials worthy of commercial availability are far from being viable. Optimization of complementary physical properties (e.g., electrical conductivity and colloidal stability) have also remained impossible in some instances. However, considering the progress of research in this field to date, it can be concluded that these materials will be commercially available in near future and their appropriate utilizations will give a long leap to materials science.

**Acknowledgment.** R.G. sincerely acknowledges the financial assistance from CSIR.

### References

- (1) Special Issue on Nanostructured Materials. *Chem. Mater.* **1996**, *8* (8), 1569–2194 and references therein
- (2) Tasi, H.-L.; Schindler, J. L.; Kannewurf, C. R.; Kanatzidis, M. G. *Chem. Mater.* **1997**, *9*, 875.
- (3) Nazar, L. F.; Zhang, Z.; Zinkweg, D. *J. Am. Chem. Soc.*, **1992**, *114*, 6239.
- (4) Vassilion, J. K.; Ziebarth, R. P.; Disalvo, F. J. *Chem. Mater.* **1990**, *2*, 738.

- (5) Beecroft, L. L.; Ober, C. K. *Chem. Mater.* **1999**, *9*, 1302 and references therein.
- (6) Cao, G.; Garcia, M. E.; Aleala, M.; Burgess, L. F.; Mallouk, T. E. *J. Am. Chem. Soc.* **1992**, *114*, 7574.
- (7) Martin, C. R. *Chem. Mater.* **1996**, *8*, 1739.
- (8) (a) Ruiz-Hitzky, E. *Adv. Mater.* **1993**, *5*, 334. (b) Ruiz-Hitzky, E.; Aranda, P. *An. Quim. Int. Ed.* **1997**, *93*, 197.
- (9) Armes, S. P.; Gottesfeld, S.; Beery, J. G.; Garzon, F.; Agnew, S. F. *Polymer* **1991**, *32*, 2325.
- (10) Gill, M.; Mykytiuk, J.; Armes, S. P.; Edwards, J. L.; Yeats, T.; Moreland, P.; Mollett, C. *J. Chem. Soc., Chem Commun.* **1992**, 108.
- (11) (a) Gill, M.; Armes, S. P.; Fairhurst, D.; Emmett, S. N.; Idzorek, G.; Pigott, T. *Langmuir* **1992**, *8*, 2178. (b) Stejskal, J.; Kratochvil, P.; Armes, S. P.; Lascelles, S. F.; Riede, A.; Helmstedt, M.; Prokes, J.; Krivka, I. *Macromolecules* **1996**, *29*, 6814.
- (12) Terrill, N. J.; Crowley, T.; Gill, M.; Armes, S. P. *Langmuir* **1993**, *9*, 2093.
- (13) Maeda, S.; Armes, S. P. *J. Colloid Interface Sci.* **1993**, *159*, 257.
- (14) Maeda, S.; Armes, S. P. *J. Mater. Chem.* **1994**, *4*, 935.
- (15) Maeda, S.; Armes, S. P. *Synth. Met.* **1995**, *69*, 499.
- (16) Maeda, S.; Armes, S. P. *Chem. Mater.* **1995**, *7*, 171.
- (17) Flitton, R.; Johal, J.; Maeda, S.; Armes, S. P. *J. Colloid Interface Sci.* **1995**, *173*, 135.
- (18) Maeda, S.; Armes, S. P. *Synth. Met.* **1995**, *73*, 151.
- (19) Perruchot, C.; Chehimi, M. M.; Delamar, M.; Lascelles, S. F.; Armes, S. P. *J. Colloid Interface Sci.* **1997**, *193*, 190.
- (20) Maeda, S.; Gill, M.; Armes, S. P.; Fletcher, I. W. *Langmuir* **1995**, *11*, 1899.
- (21) (a) Butterworth, M. D.; Corradi, R.; Johal, J.; Lascelles, S. F.; Maeda, S.; Armes, S. P. *J. Colloid Interface Sci.* **1995**, *174*, 510. (b) Lascelles, S. F.; McCarthy, G. P.; Butterworth, M. D.; Armes, S. P. *Colloid Polym. Sci.* **1998**, *276*, 893.
- (22) Azioune, A.; Pech, K.; Souidi, B.; Chehimi, M. M.; McCarthy, G. P.; Armes, S. P. *Synth. Met.* **1999**, *102*, 1419.
- (23) Partch, R.; Gangolli, S. G.; Matijevic, E.; Cai, W.; Aaraj, S. *J. Colloid Interface Sci.* **1991**, *144*, 27.
- (24) Huang, C. L.; Partch, R. E.; Matijevic, E. *J. Colloid Interface Sci.* **1995**, *170*, 275.
- (25) Huang, C. L.; Matijevic, E. *J. Mater. Res.* **1995**, *10*, 1327.
- (26) Biswas, M.; Ray, S. S.; Liu, Y. *Synth. Met.* **1999**, *105*, 99.
- (27) Gan, L. M.; Zhang, L. H.; Chan, H. S. O.; Chew, C. H. *Mater. Chem. Phys.* **1995**, *40*, 94.
- (28) Selvan, S. T. *Chem. Commun.* **1998**, 351.
- (29) Selvan, S. T.; Spatz, J. P.; Klok, H. A.; Moller, M. *Adv. Mater.* **1998**, *10*, 132.
- (30) Marinakos, S. M.; Brousseau, L. C., III; Jones, A.; Feldheim, D. L. *Chem. Mater.* **1998**, *10*, 1214.
- (31) Bhattacharya, A.; Ganguly, K. M.; De, A.; Sarkar, S. *Mater. Res. Bull.* **1996**, *31*, 527.
- (32) Gangopadhyay, R.; De, A. *Eur. Polym. J.* **1999**, *35*, 1985.
- (33) Ray, S. S.; Biswas, M. *Mater. Res. Bull.* **1998**, *33*, 533.
- (34) Baraton, M. I.; Merhari, L.; Wang, J.; Gonsalves, K. E. *Nanotechnology* **1998**, *9*, 356.
- (35) Hori, T.; Kuramoto, N.; Tagaya, H.; Karasu, M.; Kadokawa, J. I.; Chiba, K. *J. Mater. Res.* **1999**, *14*, 5.
- (36) (a) Wampler, W. A.; Rajeshwar, K.; Pethe, R. G.; Hyer, R. C.; Sharma, S. C. *J. Mater. Res.* **1995**, *10*, 1811. (b) Wampler, W. A.; Basak, S.; Rajeshwar, K. *Carbon* **1996**, *34*, 747.
- (37) Gangopadhyay, R.; De, A.; Das, S. N. *J. Appl. Phys.* **2000**, March 1, 87, in press.
- (38) Kryszewski, M.; Jeszka, J. K. *Synth. Met.* **1998**, *94*, 99.
- (39) Butterworth, M. D.; Armes, S. P.; Simpson, A. W. *J. Chem. Soc., Chem. Commun.* **1994**, 2129.
- (40) Butterworth, M. D.; Bell, S. A.; Armes, S. P.; Simpson, A. W. *J. Colloid Interface Sci.* **1996**, *183*, 91.
- (41) Philipse, A. P.; van Bruggen, M. P. B.; Pathmamonoharan, C. *Langmuir* **1994**, *10*, 92.
- (42) Nguyen M. T.; Diaz, A. *Adv. Mater.* **1994**, *6*, 858.
- (43) Wan, M.; Zhou, W.; Li, J. *Synth. Met.* **1996**, *78*, 27.
- (44) Wan, M.; Li, J. *J. Polym. Sci.: Part A: Polym. Chem.* **1998**, *36*, 2799.
- (45) Wan, M.; Fan, J. *J. Polym. Sci.: Part A: Polym. Chem.* **1998**, *36*, 2749.
- (46) Tang, B. Z.; Geng, Y.; Lam, J. W. Y.; Li, B.; Jing, X.; Wang, X.; Wang, F.; Pakhomov, A. B.; Zhang, X. X. *Chem. Mater.* **1999**, *11*, 1581.
- (47) Pokhodenko, V. D.; Krylov, V. A.; Kurys, Y. I.; Posudievsky, O. Y. *Phys. Chem. Chem. Phys.* **1999**, *1*, 905.
- (48) Miyauchi, S. N.; Abiko, H.; Sorimachi, Y.; Tsubata, I. *J. Appl. Polym. Sci.* **1989**, *37*, 289.
- (49) (a) Somani, P.; Kale, B. B.; Amalnerkar, D. P. *Synth. Met.* **1999**, *106*, 53. (b) Somani, P. R.; Marimuthu, R.; Mulik, U. P.; Sainkar, S. R.; Amalnerkar, D. P. *Synth. Met.* **1999**, *106*, 53.
- (50) Cantu, M. L.; Romero, P. G. *Chem. Mater.* **1998**, *10*, 698.
- (51) Gemeay, A. H.; Nishiyama, H.; Kuwabata, S.; Yoneyama, H. *J. Electrochem. Soc.* **1995**, *142*, 4190.
- (52) Kuwabata, S.; Idzu, T.; Martin, C. R.; Yoneyama, H. *J. Electrochem. Soc.* **1998**, *145*, 2707.
- (53) Qi, Z.; Pickup, P. G. *Chem. Commun.* **1998**, 15.
- (54) Qi, Z.; Pickup, P. G. *Chem. Commun.* **1998**, 2299.
- (55) Qi, Z.; Lefebvre, M. C.; Pickup, P. G. *Electroanal. Chem.* **1998**, *459*, 9.
- (56) (a) Huang, S. W.; Neoh, K. G.; Kang, E. T.; Han, H. S.; Tan, K. L. *J. Mater. Chem.* **1998**, *8*, 1743. (b) Huang, S. W.; Neoh, K. G.; Shih, C. W.; Lim, D. S.; Kang, E. T.; Han, H. S.; Tan, K. L. *Synth. Met.* **1998**, *96*, 117.
- (57) Neoh, K. G.; Tan, K. K.; Goh, P. L.; Huang, S. W.; Kang, E. T.; Tan, K. L. *Polymer* **1999**, *40*, 887.
- (58) Drelinkiewicz, A.; Hasik, M.; Choczynski, M. *Mater. Res. Bull.* **1998**, *33*, 739.
- (59) Chriswanto, H.; Ge, H.; Wallace, G. G. *Chromatographia* **1993**, *37*, 423.
- (60) Chriswanto, H.; Wallace, G. G. *Chromatographia* **1996**, *42*, 191.
- (61) Perruchot, C.; Chehimi, M. M.; Delamar, M.; Fievet, F. *Surf. Interface Anal.* **1998**, *26*, 689.
- (62) Perruchot, C.; Chehimi, M. M.; Mordenti, D.; Briand, M.; Delamar, M. *Surf. Interface Anal.* **1998**, *8*, 2185.
- (63) Faverolle, F.; Le Bars, O.; Attias, A. J.; Bloch, B. *J. Chim. Phys.* **1995**, *92*, 943.
- (64) Faverolle, F.; Le Bars, O.; Attias, A. J.; Bloch, B. *Organic Coatings*; Lacaze, P. C., Ed.; Woodbury: New York, 1996; p 267.
- (65) Goodwin, J. W.; Habron, R. S.; Reynolds, P. A. *Colloid Polym. Sci.* **1990**, *268*, 766.
- (66) Philippe, A. P.; Vrig, A. *Colloid Interface Sci.* **1994**, *165*, 519.
- (67) Maeda, S.; Corradi, R.; Armes, S. P. *Macromolecules* **1995**, *28*, 2905.
- (68) Tarcha, P. J.; Misun, D.; Finley, D.; Wong, M.; Donovan, J. J. *Polymer Latexes, Preparation, Characterisation and Applications*; Daniels, E. S., Sudol, E. d., El-assar, M. S., Eds.; ACS Symp. Ser. 492, American Chemical Society: Washington, DC, 1992; p 347.
- (69) Pope, M. R.; Armes, S. P.; Tarcha, P. J. *Bioconjugate Chem.* **1996**, *7*, 436.
- (70) McCarthy, G. P.; Armes, S. P.; Greaves, S. J.; Watts, J. F. *Langmuir* **1997**, *13*, 3686.
- (71) Saoudi, B.; Jammul, N.; Chehimi, M. M.; McCarthy, G. P.; Armes, S. P. *J. Colloid Interface Sci.* **1997**, *192*, 269.
- (72) Goller, M. I.; Barthet, C.; McCarthy, G. P.; Corradi, R.; Newby, B. P.; Wilson, S. A.; Armes, S. P.; Luk, S. Y. *Colloid Polym. Sci.* **1998**, *276*, 1010.
- (73) Yoneyama, H.; Shoji, Y.; Kawai, K. *Chem. Lett.* **1989**, 1067.
- (74) Ikeda, O.; Yoneyama, H. *J. Electroanal. Chem.* **1989**, *265*, 323.
- (75) Ogura, K.; Endo, N.; Nakayama, M. *J. Electrochem. Soc.* **1998**, *145*, 3801.
- (76) Kawai, K.; Mihara, N.; Kuwabata, S.; Armes, S. P. *J. Electrochem. Soc.* **1990**, *137*, 1793.
- (77) Yoneyama, H.; Shoji, Y. *J. Electrochem. Soc.* **1990**, *137*, 3826.
- (78) Wang, G.; Chen, H.; Zhang, H.; Shen, Y.; Yuan, C.; Z. C. Lu, C.; Wang, G.; Yang, W. *Phys. Lett. A* **1998**, *237*, 165.
- (79) Yoneyama, H.; Kishimoto, A.; Kuwabata, S. *J. Chem. Soc., Chem. Commun.* **1991**, 986.
- (80) Kuwabata, S.; Kishimoto, A.; Tanaka, T.; Yoneyama, H. *J. Electrochem. Soc.* **1994**, *141*, 10.
- (81) Takamura, T.; Nagashima, M.; Mine, T.; Tamura, I.; Ikeshawa, Y. Proceedings of the 35th Int. Power Sources Symp., Cherry Hill, NJ, 1992, p 187.
- (82) (a) Wampler, W. A.; Wei, C.; Rajeswar, K. *J. Electrochem. Soc.* **1994**, *141*, L13. (b) Wampler, W. A.; Wei, C.; Rajeswar, K. *J. Mater. Res.* **1995**, *7*, 585.
- (83) Wei, C.; German, S.; Basak, S.; Rajeshwar, K. *J. Electrochem. Soc.* **1993**, *140*, L60.
- (84) Zhang, P.; Yang, Z. H.; Wang, D. J.; Kan, S. H.; Chai, X. D.; Liu, J. Z.; Li, T. *J. Synth. Met.* **1997**, *84*, 165.
- (85) Shen, P. K.; Huang, H. T.; Tseung, C. C. *J. Electrochem. Soc.* **1992**, *139*, 1840.
- (86) Komaba, S.; Fujihana, K.; Osaka, T.; Aiki, S.; Nakamura, S. *J. Electrochem. Soc.* **1998**, *145*, 1126.
- (87) Aboutaneos, V.; Barisci, J. N.; Kane-Maguir, L. A. P.; Wallace, G. G. *Synth. Met.* **1999**, *106*, 89.
- (88) Hable, C. T.; Wrighton, M. S. *Langmuir* **1991**, *7*, 1305.
- (89) Esteban, P. O.; Leger, J. M.; Lamy, C.; Genies, E. *J. Appl. Electrochem.* **1989**, *19*, 462.
- (90) Swathirajan, S.; Mikhail, Y. M. *J. Electrochem. Soc.* **1992**, *139*, 2105.
- (91) Athawale, A. A.; Deore, B. Proceedings of Polymers '99: Int. Symp. on Polymers Beyond AD 2000, New Delhi, India, 1999; p 792.
- (92) Torsi, L.; Pezzuto, M.; Siciliano, P.; Rella, R.; Sabbatini, L.; Valli, L.; Zamboni, P. G. *Sensors Actuators B, Chem.* **1998**, *48*, 362.
- (93) (a) Bidan, G.; Jarjayes, O.; Fruchart, J. M.; Hannecart, E. *Adv. Mater.* **1994**, *6*, 152. (b) Jarjayes, O.; Fries, P. H.; Bidan, G. *Synth. Met.* **1995**, *69*, 343.
- (94) Jarjayes, O.; Fries, P. H.; Bidan, G. *J. Magn. Magn. Mater.* **1994**, *137*, 205.
- (95) Jarjayes, O.; Auric, P. *J. Magn. Magn. Mater.* **1994**, *138*, 115.